Vol 17 No 4, April 2008
1674-1056/2008/17(04)/1305-07

Chinese Physics B

© 2008 Chin. Phys. Soc.
and IOP Publishing Ltd

# Comparison of the mechanism of gap formation for tri- and bi-component phononic crystal*

Zhao Hong-Gang(赵宏刚)†, Wen Ji-Hong(温激鸿), Liu Yao-Zong(刘耀宗), Yu Dian-Long(郁殿龙), Wang Gang(王 刚), and Wen Xi-Sen(温熙森)

*Institute of Mechatronical Engineering, National University of Defense Technology, Changsha* 410073, *China*

(Received 18 May 2007; revised manuscript received 22 June 2007)

Using an exact Mie scattering solution, this paper investigates the mode conversions during the Mie scattering of a single bi- or one-component sphere in unbounded epoxy. Then the formation mechanism of the first complete gap in the corresponding tri- or bi-component phononic crystal is investigated by the multiple-scattering method. It is shown that the heavy density of the scatterer plays an essential role in the Mie resonance and the formation of the gaps for both types of the phononic crystals. For the tri-component phononic crystal, the gap is mainly induced by the Mie resonance of the single scatterer. For the bi-component phononic crystal, the transverse wave (by mode-conversion during the Mie scattering under a longitudinal wave incidence) is modulated by the periodicity and governed by the Bloch theory, which induces the gap cooperatively.

**Keywords:** phononic crystal, Mie scattering, multiple scattering, band gap
**PACC:** 4320, 6780C, 4340

## 1. Introduction

The propagation of elastic wave in periodic composite materials, known as phononic crystals (PCs), has received much attention in the last decade.[1−19] Within PCs the density and/or elastic coefficients vary periodically in space. Under certain conditions, the PC can exhibit a phononic band gap (PBG). The PBG is a frequency domain where the propagation of elastic wave is forbidden.[5,6] Analogous to photonic crystal, it is generally known that the PBG is induced jointly by the Mie scattering and the periodicity.[7] For solid PCs, there are several wave polarizations, i.e. one longitudinal and two transverse waves, which lead to some difficulties in explaining the mechanism of the gap formation. Refs.[8, 9] investigated the relationship between the band gaps and the Mie scattering of a single inclusion. The results showed that the gap may appear in the frequency region between the separated Mie resonances. Some authors[10,11] focused their studies on the lowest complete band gap. The results showed that the gaps were opened by the interaction between the rigid body resonance (RBR, denoted by the first peak of the normalized scattering cross-section[12]) and the effective homogeneous medium. All the above studies focused on bi-component PCs. Among them, the roles of the periodicity and the coupling between the longitudinal and transverse waves were not carefully considered. The main goal of the present paper is comparing the mechanism of the gap formation for tri- and bi-component PCs by considering both the Mie resonance and the periodicity. The Mie scattering and the multiple-scattering method are adopted during the investigations.

## 2. Theoretical models and multiple-scattering method

### 2.1. Theoretical models

We consider a PC composed of a simple cubic lattice of nonoverlapping spheres with radius $R$, embedded in a continuous host. Figure 1 shows the model of the three-dimensional PC considered in this paper under the Cartesian coordinate system. The intra-layer spheres on the $XY$ plane are arranged infinitely in a two-dimensional square lattice defined by the primitive vectors $\boldsymbol{a}_1$ and $\boldsymbol{a}_2$ (see Fig.1(a)). Figure 1(b) shows the first Brillouin zone correspondingly. The fi-

*Project supported by the State Key Development Program for Basic Research of China (Grant No 51307) and the National Natural Science Foundation of China (Grant No 50575222).
†E-mail: zhhg9603@yahoo.com.cn

nite crystal slab can be viewed as a sequence of planes of spheres perpendicular to the $Z$ axis (see Fig.1(c)). For simplicity, the slab extends infinitely on both sides in order to avoid the interfacial scattering. A plane wave is incident from the left host, and accordingly the transmittance is close to 1 at low frequency range.

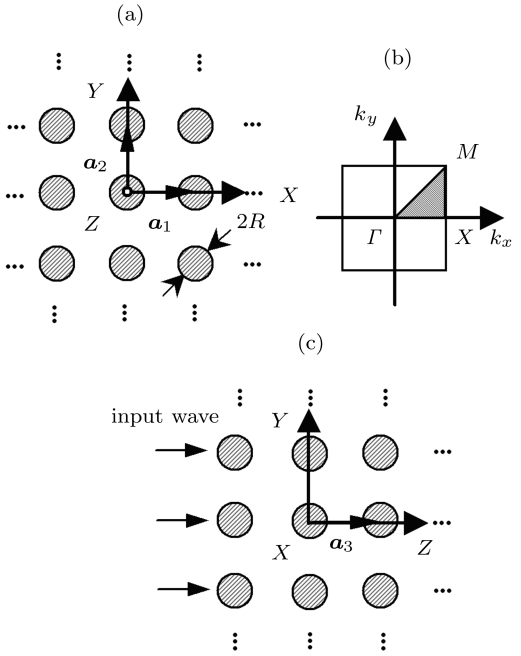



**Fig.1.** A PC composed of a simple cubic lattice, denoted by primitive vectors $\boldsymbol{a}_1$, $\boldsymbol{a}_2$ and $\boldsymbol{a}_3$, of nonoverlapping spheres with radius $R$ embedded in continuous host. (a) The lattice in the intra-layer. (b) The first unreduced Brillouin zone of the lattice in the intra-layer. (c) The lattice in the inter-layer. For the finite slab, a plane wave is incident from the left.

## 2.2. Multiple-scattering method

The displacement in a homogeneous elastic medium is represented by the following time-independent equation:

$$(\lambda + 2\mu)\nabla(\nabla \cdot \boldsymbol{u}) - \mu\nabla \times \nabla \times \boldsymbol{u} + \rho\omega^2\boldsymbol{u} = 0. \quad (1)$$

In a spherical coordinate system, the solution can be decomposed into one longitudinal and two transverse solutions:[13,14]

$$\boldsymbol{u} = \boldsymbol{L} + \boldsymbol{M} + \boldsymbol{N}. \quad (2)$$

The process of obtaining the Mie scattering matrix of a coated sphere is an eigenfunction expansion of the displacement fields in each component. The fields are composed of infinite summations of spherical harmonics with unknown modal coefficients:

$$\boldsymbol{u}(\boldsymbol{r}) = \sum_{lm\sigma} \left[a_{lm\sigma}\boldsymbol{J}_{lm\sigma}(\boldsymbol{r}) + b_{lm\sigma}\boldsymbol{H}_{lm\sigma}(\boldsymbol{r})\right], \quad (3)$$

where $\sigma = 1, 2, 3$ correspond to $\boldsymbol{L}$, $\boldsymbol{M}$, $\boldsymbol{N}$ modes respectively. The definitions of $\boldsymbol{J}_{lm\sigma}(\boldsymbol{r})$ and $\boldsymbol{H}_{lm\sigma}(\boldsymbol{r})$ can be found in Ref.[13]; $b_{lm\sigma}, a_{lm\sigma}$ represent the expansion coefficients of the scattered and input waves respectively. Then, the boundary conditions, i.e. the displacement and stress continuity at the inner and outer interfaces of the coating layer, lead to 12 linear equations. The solution of these equations gives the relations between the scattered and input waves, with the modal coefficients $B = \{b_{lm\sigma}\}$ and $A = \{a_{lm\sigma}\}$ respectively. The relation between the coefficients $B = \{b_{lm\sigma}\}$ and $A = \{a_{lm\sigma}\}$ reveals the following scattering matrix form:

$$B = TA, \quad (4)$$

where $T = \{t_{lm\sigma l'm'\sigma'}\}$. For spherical scatterer, the scattering matrix is independent of $m$ and diagonal with the spherical-wave expansion order $l$. The scattering matrix for each $l$ has the following form:

$$T_l = \begin{bmatrix} LL & 0 & LN \\ 0 & MM & 0 \\ NL & 0 & NN \end{bmatrix}. \quad (5)$$

The meanings of the five nonzero elements are pellucid. For example, $LL$ stands for a longitudinal incident wave scattered into a longitudinal outgoing wave. It shows that the $\boldsymbol{L}$ mode and the $\boldsymbol{N}$ mode are coupled to each other, while the $\boldsymbol{M}$ mode is decoupled.

The multiple-scattering method is a layer-by-layer approach for calculating the transmittance and reflectance for a finite slab with layers of scatterers. For one scatterer in a plane of scatterers, the scattered wave,

$$\boldsymbol{u}^{\mathrm{sc}}(\boldsymbol{r}) = \sum_{lm\sigma} b_{lm\sigma}\boldsymbol{H}_{lm\sigma}(\boldsymbol{r}), \quad (6)$$

is completely determined by the overall incident waves, which include two parts. One is the externally incident wave $\boldsymbol{u}^{\mathrm{in(e)}}(\boldsymbol{r}) = \sum_{lm\sigma} a^{(\mathrm{e})}_{lm\sigma}\boldsymbol{J}_{lm\sigma}(\boldsymbol{r})$. The second part is the sum of all the scattered waves except that from the considered scatterer. We obtain

$$\boldsymbol{u}^{\mathrm{in}}(\boldsymbol{r}) - \boldsymbol{u}^{\mathrm{in(e)}}(\boldsymbol{r}) = \sum_{\boldsymbol{R}_j \neq 0} \sum_{lm\sigma} b^j_{lm\sigma}\boldsymbol{H}^j_{lm\sigma}(\boldsymbol{r}_j), \quad (7)$$

where $\boldsymbol{r}_j$ refers to the position of the spatial point measured from scatterer $j$, and $\boldsymbol{R}_j$ represents the position of scatterer $j$. According to the Bloch theorem, one obtains

$$b^j_{lm\sigma} = b_{lm\sigma}\exp(\mathrm{i}\boldsymbol{k}_{//} \cdot \boldsymbol{R}_j), \quad (8)$$

where $\boldsymbol{k}_{//}$ is a reduced wave vector in the 2D Brillouin zone of the reciprocal lattice. The coefficients of $\{b_{lm\sigma}\}$ are completely determined by $\left\{a^{(e)}_{lm\sigma}\right\}$ through the scattering matrix $T$.

To get the transmittance and reflectance of the PC slab including the monolayer scatterers, all the expansions of spherical waves of total input and output waves need to be transformed to plane waves. Then we can obtain the relations of the input and output waves for the slab containing the monolayer scatterers as follows:

$$\boldsymbol{U}^{+}(N+1) = \boldsymbol{Q}^{\mathrm{I}}\boldsymbol{U}^{+}(N) + \boldsymbol{Q}^{\mathrm{II}}\boldsymbol{U}^{-}(N+1), \quad (9a)$$

$$\boldsymbol{U}^{-}(N) = \boldsymbol{Q}^{\mathrm{III}}\boldsymbol{U}^{+}(N) + \boldsymbol{Q}^{\mathrm{IV}}\boldsymbol{U}^{-}(N+1). \quad (9b)$$

The superscript $+(-)$ means that the incidence is along positive (negative) $Z$-axis. For details one can refer to Refs.[13, 14]. Once the matrices $Q$ for one scattering layer are determined, one can easily obtain the $Q$ matrices of a slab of $N$ layers thick. As for the inter-layer periodicity along the $Z$-axis, the Bloch-theory guarantees

$$\boldsymbol{U}^{\pm}(N+1) = \exp(\mathrm{i}\boldsymbol{k}\cdot\boldsymbol{a}_3)\boldsymbol{U}^{\pm}(N), \quad (10)$$

where $\boldsymbol{a}_3$ is the primitive vector along positive $Z$-axis [see Fig.1(c)], $\boldsymbol{k} = (\boldsymbol{k}_{//}, \boldsymbol{k}_{\boldsymbol{z}}(\omega, \boldsymbol{k}_{//}))$. After some algebra it yields a standard eigenfunction:

$$\begin{pmatrix} \boldsymbol{Q}^{\mathrm{I}} & \boldsymbol{Q}^{\mathrm{II}} \\ -\left[\boldsymbol{Q}^{\mathrm{IV}}\right]^{-1}\boldsymbol{Q}^{\mathrm{III}}\boldsymbol{Q}^{\mathrm{I}} & \left[\boldsymbol{Q}^{\mathrm{IV}}\right]^{-1}\left[\boldsymbol{I} - \boldsymbol{Q}^{\mathrm{III}}\boldsymbol{Q}^{\mathrm{II}}\right] \end{pmatrix} \begin{pmatrix} \boldsymbol{U}^{+}(N) \\ \boldsymbol{U}^{-}(N+1) \end{pmatrix} = \exp(\mathrm{i}\boldsymbol{k}\cdot\boldsymbol{a}_3) \begin{pmatrix} \boldsymbol{U}^{+}(N) \\ \boldsymbol{U}^{-}(N+1) \end{pmatrix}, \quad (11)$$

where $\boldsymbol{I}$ is an unit matrix. For given $\boldsymbol{k}_{//}$ and $\omega$, we can obtain the eigenvalues $\boldsymbol{k}_{\boldsymbol{z}}(\omega, \boldsymbol{k}_{//})$.

## 3. Results and discussions

Since the $T$ matrix is independent of $m$ and is diagonal with expansion order $l$, we can consider the partial wave of $l$ order separately. Figure 2(c) shows the absolute values of the $T$-matrix elements of $l = 1$ (i.e, $T_1$, denotes the dipole partial wave) for a single Pb sphere coated by silicon rubber embedded in epoxy. The core and the coated radii are $R_1 = 5.25\,\mathrm{mm}$ and $R = 6.75\,\mathrm{mm}$ respectively. The lattice constant in the present and the following computations is 15 mm. The frequency resolution used here is 1.5 Hz. The parameters of the components denoted by the density ($\rho$),

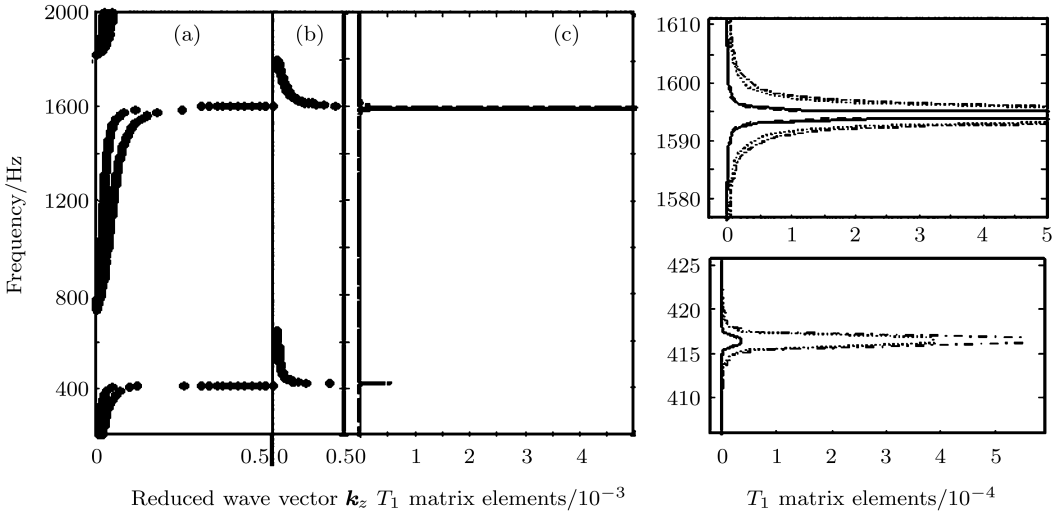



**Fig.2.** The real (a) and imaginary (b) parts of $\boldsymbol{k}_{\boldsymbol{z}}$, i.e., the complex band structure, of the PC composed of simple cubic lattice of Pb spheres ($R_1 = 5.25\,\mathrm{mm}$) coated by silicon rubber ($R = 6.75\,\mathrm{mm}$) embedded in epoxy. (c) The amplitudes of the elements in the $T_1$ for a single coated Pb sphere. The right presents the corresponding zooms of the sharp resonances. The amplitude of the $\boldsymbol{L}$ mode to $\boldsymbol{L}$ ($\boldsymbol{N}$) mode is plotted by dashed (solid) line, and $\boldsymbol{N}$ mode to $\boldsymbol{L}$ ($\boldsymbol{N}$) mode by dotted (dashed dotted) line.

longitudinal wave speed ($c_{\rm l}$) and transverse wave speed ($c_{\rm t}$) are listed in Table 1. For the low-frequency range of interest, we find that only the elements in $T_1$ have obvious amplitudes, so the plots for the $T$-matrices of other partial waves are omitted. A notable feature is the severe resonances, denoted by the sharp peaks in the plots (the sharpness of the peaks implies a long lifetime of the resonance). The *LL*, *NL*, *LN* and *NN* resonances (unfortunately, we find no obvious resonance in *MM* mode) occur at the same frequency, around 504 Hz and 1591 Hz, respectively. Figures 2(a) and 2(b) show the real and imaginary parts of $\boldsymbol{k_z}$ vs. frequency, i.e. the complex band structure, of the corresponding PC composed of a simple cubic lattice of the coated Pb spheres embedded in epoxy. From Fig.2(b), we can see that the intense attenuation occurs just above the resonant frequency, which is induced by the so-called Fano-like phenomenon.[15] Comparing Fig.2(a) with Fig.2(c), one can see that the Mie resonances give rise to the relatively flat bands at the bottom of the first and second gaps. Here we pay more attention to the low frequency resonance, in which the core sphere resonates as a whole. The physical insight of this resonance can be explained by a mass-spring model denoted by an analytic formula.[16−19] Note that the periodicity may play little role in the gap formation because the wavelength near the gap is much larger than the lattice. As verification, the almost linear dispersion in Fig.2(a) above the first gap denotes that the three-component PC behaves like an effective medium. When reaching the Mie resonance, the coupling between the linear dispersion and the resonance of the individual sphere opens the first complete gap, which exists between 504 Hz and 802 Hz. So the mechanism of the lowest gap formation emerges as the interaction of the sharp Mie resonance and the effective medium. We further investigate the effects of the core mass on the Mie resonance. It shows that the low-frequency resonance (and the first complete gap) disappears gradually when the density of the core is artificially decreased.

**Table 1.** Physical parameters of the materials.

| Material | $\rho$/kgm$^{-3}$ | $c_l$/ms$^{-1}$ | $c_{\rm t}$/ms$^{-1}$ |
|---|---|---|---|
| Pb | 11600 | 2493 | 1133 |
| Epoxy | 1180 | 2490 | 1180 |
| Silicon rubber | 1300 | 22.8 | 5.5 |

Then we replace the rigid host of the PC discussed above with soft silicon rubber: i.e., forming a binary PC correspondingly. Great changes appear in the shapes of the plots for the $T$ elements. The sharp peaks disappear (see Figs.3(c) and 3(d)), accordingly the flat bands are replaced by the wide ones in the band structure, as shown in Fig.3(a). From Fig.3(d), one can see that the amplitudes of the elements in the $T$-matrix of $l = 2$ (i.e, $T_2$, denotes the quadrupole partial wave) are almost the same as those in $T_1$. The remarkable amplitudes of the elements in $T_2$, however,

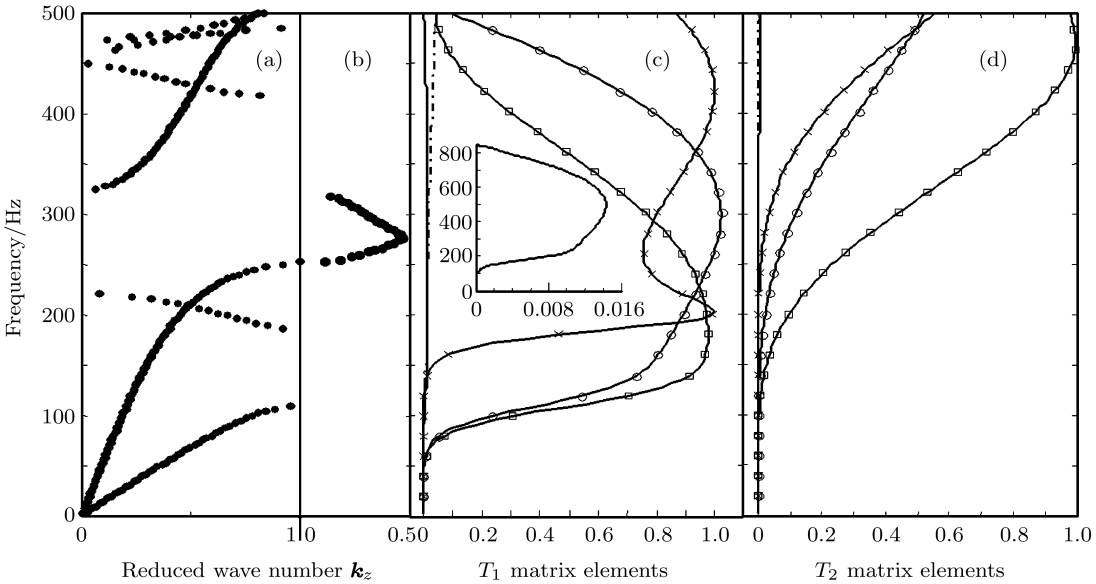



**Fig.3.** The real (a) and imaginary (b) parts of $\boldsymbol{k_z}$ for the binary PC by replacing the epoxy host of the tri-component PC with silicon rubber. The amplitudes of the *LN*, *LL*, *MM*, *NL* and *NN* modes are plotted by the solid, dashed doted, solid lines with crosses, circles and squares respectively: (c), $T_1$, (d), $T_2$. The inset in (c) shows the panorama of the first resonance of *LN* mode.

are above the first complete gap between 253 Hz and 320 Hz. We may conclude that this complete gap is mainly induced by the Mie scattering of the dipole partial wave. In detail, one can see that there is *MM* resonance near 200 Hz in $T_1$, which induces the relative flat band between 180 Hz and 220 Hz. Other elements in $T_1$ hold remarkable amplitudes, however, no obvious peaks correspond to the flat bands at the bottom and the top of the gap. The reason may be that the wavelength near the gap is comparable to the lattice constant. The periodicity in the PC must be considered carefully.

As with the model built in Section 2, the periodicity can be considered as the intra-layer ($XY$ plane) and inter-layer types. We consider the former firstly. For longitudinal wave incidence, it can be seen that the longitudinal wave doses the substantial mode conversion into transverse wave during the Mie scattering, denoted by the *LN* mode (see the insertion in Fig.3(c)). Note that the longitudinal wavelength is 4.1 times of that of the transverse wave in silicon rubber. The transverse wave interaction among the lattice will dominate the transmittance of the longitudinal wave in the low frequency range. The transverse wave, originated from the mode conversion from the incident longitudinal wave, is modulated by the intra-layer periodicity and satisfies the Bloch theory. Below the first Bloch frequency [i.e., $\Omega = fa/c_{\rm t} = 1$, with a frequency 367 Hz denoted by the arrow in Fig.4(a)] the destructive interface for the transverse wave interaction enhances the dipole resonance of the scatterer, which represents a 'rigid body translational dipole resonance'.[12] The destructive interaction of the transverse waves blocks the wave transmission. From Fig.4(a), we can readily see that the transmittance dip exists around 270 Hz in the monolayer slab. For finite multilayer slabs, a series of such attenuation dips will lead to zero of transmission into gap. One can apply a similar analysis to the case of transverse incidence. From Fig.4(b), one can see that the dip (gap) of the monolayer (multilayer) slab for transverse wave incidence is wider than that of the longitudinal wave incidence. A reasonable explanation is offered next.

Now, we artificially reduce the density of Pb sphere and let it possess the same density as the host. The other parameters, however, are kept unchanged. We denote this artificial material as D. From Fig.5(b), one can see that the low frequency resonance in $T_1$ disappears. Accordingly the mode conversion occurs

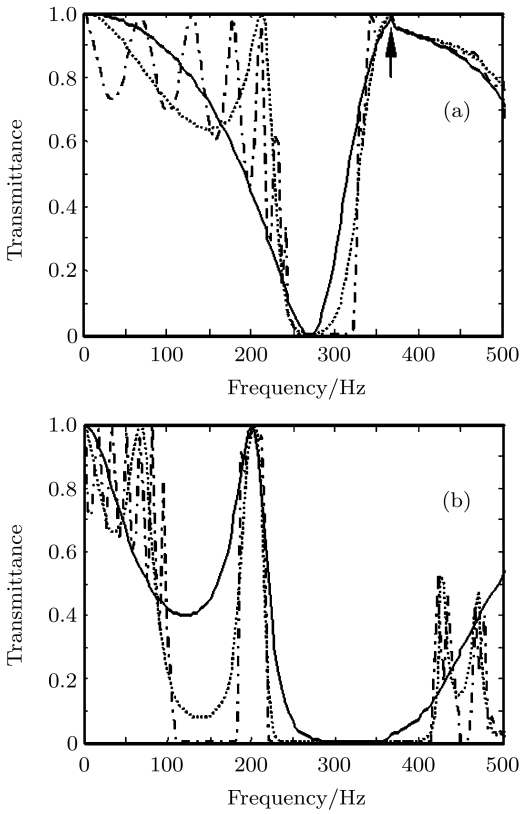



**Fig.4.** Transmittances of incident longitudinal (a) and transverse (b) waves through finite bi-component PC slabs. The slabs are 1 (solid line), 2 (dotted line) and 8 (dashed dotted line) layers thick respectively. The arrow in (a) denotes the first Bloch frequency. Each layer is 15 mm thick.

from longitudinal wave to transverse wave, then the "dipole" resonance vanishes. One can readily see that no complete gap exists in the band structure, as shown in Fig.5(a). So the PC containing scatterer D serves as a good sample to investigate the gap induced only by the inter-layer periodicity. According to the condition of the Bragg reflection, there is a well-known approximation equation for the centre frequency of the gap, i.e.,

$$\Psi_i = fa/c_i = n/2, \quad n = 1, 2, \cdots, \tag{12}$$

where $c_i$ is the velocity of the host, and the subscript $i$ =l,t represent the longitudinal and transverse waves respectively. The first longitudinal gap, around 760 Hz given by Eq.(12), is beyond the frequency range considered here. So there is no obvious dips or gaps in Fig.6(a). For transverse wave incidence, it can be seen from Fig.6(b) that there exist two gaps around 215 Hz and 390 Hz respectively. These gaps correspond to, but are little higher than the first and second gaps around 183 Hz and 367 Hz predicted by Eq.(12)

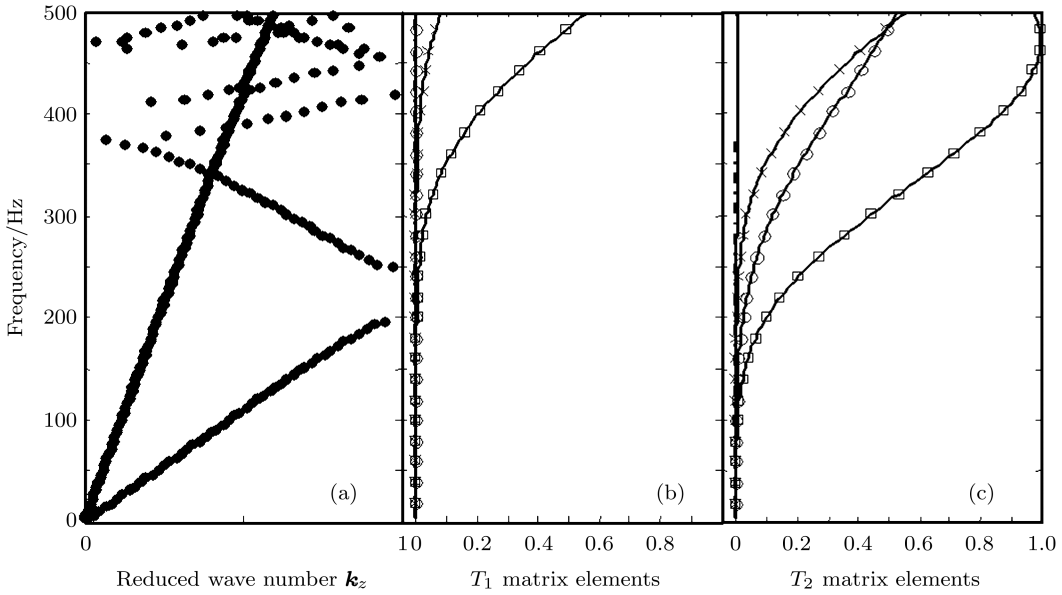



**Fig.5.** As Fig.3, except that the scatterer has the same density as silicon rubber. The *LN*, *LL*, *NL* modes in (b) and *LN*, *LL* modes in (c) are almost superposed together.

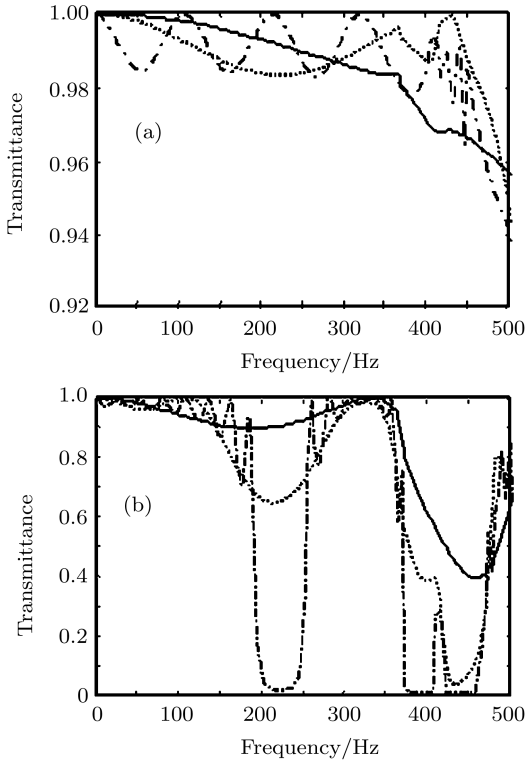



**Fig.6.** As Fig.4, except that the scatterer has the same density as silicon rubber.

respectively. The differences are mainly induced by the local spherical interface among the lattice. For Pb sphere, these two Bragg gaps (the difference is induced by the Mie resonance of Pb sphere) coalesce with the resonance gap around 300 Hz, and form a wide gap between 220 Hz and 420 Hz, as shown in Fig.4(b). The first gap from 110 Hz to 175 Hz in Fig.4(b) may be induced by the *NN* resonance of the single Pb sphere, which is beyond our consideration in this paper.

## 4. Conclusions

We have compared the formation mechanisms of the first complete gaps of the tri- and bi-component PCs. This demonstrates that the heavy density of the scatterer plays an essential role in the formation of Mie resonance and the lowest complete gap for both types of PCs. For the tri-component PC, the Mie resonance of the single sphere opens the complete gap, which is little affected by the periodicity. For the bi-component PC, the destructive interface below the first Bloch frequency for transverse wave (under a longitudinal wave incidence, the transverse wave originates from the mode conversion) blocks the wave transmission and induces the first complete gap.

# References


[1] Wu F G and Liu Y Y 2002 *Acta Phys. Sin.* **51** 1434 (in Chinese)

[2] Wang G, Wen J H, Han X Y and Zhao H G 2003 *Acta Phys. Sin.* **52** 1943 (in Chinese)

[3] Wen J H, Wang G, Liu Y Z and Yu D L 2004 *Acta Phys. Sin.* **53** 3384 (in Chinese)

[4] Wang G, Wen J H, Liu Y Z, Yu D L and Wen X S 2005 *Acta Phys. Sin.* **54** 1247 (in Chinese)

[5] Kushwaha M S, Halevi P, Dobrzynski L and Djafarirouhani B 1993 *Phys. Rev. Lett.* **71** 2022

[6] Sigalas M M and Economou E N 1992 *J. Sound Vib.* **2** 158377

[7] Cai L and Han X Y 2006 *Acta Phys. Sin.* **55** 5866 (in Chinese)

[8] Kafesaki M and Economou EN 1995 *Phys. Rev.* B **52** 13317

[9] Klironomos A D and Economou EN 1998 *Solid State Commun.* **105** 327-332

[10] Sainidou R, Stefanouand N and Modinos A 2002 *Phys. Rev.* B **66** 212301

[11] Zhao H G, Liu Y Z, Wang G, Wen J H, Yu D L, Han X Y and Wen X S 2005 *Phys. Rev.* B **72** 12301

[12] Maslov K, Kinra V K and Henderson B K 2000 *Mech. Mater.* **32** 785

[13] Liu Z Y, Chan C T and Sheng P 2002 *Phys. Rev.* B **65** 165116

[14] Sainidou R, Stefanou N, Psarobas I E and Modinos A 2005 *Comput. Phys. Commun.* **166** 197

[15] Goffaux C, Sanchez-Dehesa J, Levy Yeyati A, Lambin P, Khelif A, Vasseur J O and Djafari-Rouhani B 2002 *Phys. Rev. Lett.* **88** 225502

[16] Goffaux C and Sanchez-Dehesa J 2003 *Phys. Rev.* B **67** 144301

[17] Wang G, Shao L H, Liu Y Z and Wen J H 2006 *Chin. Phys.* **15** 1843

[18] Wang G, Liu Y Z, Wen J H and Yu D L 2006 *Chin. Phys.* **15** 407

[19] Hirsekorn M 2004 *Appl. Phys. Lett.* **84** 3364